Order in two-dimensional projections of thin amorphous three-dimensional structures

1999 J. Phys.: Condens. Matter 11 2319

(http://iopscience.iop.org/0953-8984/11/11/004)

J. Phys.: Condens. Matter **11** (1999) 2319–2336. Printed in the UK PII: S0953-8984(99)96996-5

Order in two-dimensional projections of thin amorphous three-dimensional structures

G Mountjoy†

Cavendish Laboratory, University of Cambridge, Cambridge CB3 0HE, UK

Received 26 August 1998, in final form 18 January 1999

Abstract. Two-dimensional (2D) projections underlie the technique of high resolution electron microscopy. Projections of amorphous structures are generally considered uninterpretable due to structural disorder. We have derived the relationships between the distribution functions of an amorphous three-dimensional (3D) structure and those of the corresponding 2D projection. We have confirmed the relationships using calculations on models of amorphous structures with thickness in the range from 10.6 to 43.3 Å. For example the pair and triplet distribution functions of the 2D projections show peaks corresponding to nearest neighbour distances and bond angles (respectively). The degree of order in the 2D projection decreases as thickness increases. Similar results are expected for higher order correlation functions. Thus it has been demonstrated that 2D projections of amorphous 3D structures contain a great deal of valuable structural information.

1. Introduction

Two-dimensional (2D) projections of three-dimensional (3D) structures are fundamental to the phenomenon of electron microscopy. In particular, the standard high resolution electron microscopy (HREM) technique is capable of producing atomic resolution structural images of ultra-thin samples, with thickness $t < 200$ Å [1]. In the weak phase object approximation, the image intensity in HREM images is proportional to the projection of the atomic potential convoluted with the Fourier transform of the lens contrast transfer function. Thus the structural information underlying such an image is the 2D projection of a 3D structure. Although there are well established methods for the interpretation of standard HREM images of crystals [1], their interpretation in the case of amorphous materials has been problematic, because the resolution is limited to $\geqslant 1$ Å by lens aberrations.

However, there have recently been a number of technical breakthroughs in the field of electron microscopy, which raise the future possibility of obtaining sub-Å resolution images of the projected atomic potential. The image phase problem can be solved by holography (see e.g. [2], [3]) or through-focal series reconstruction [4] and thus lead to the deconvolution of lens aberrations. Dark- field imaging in the scanning transmission electron microscope can lead to improvements in resolution by nearly a factor of two [5]. Work is in progress to decrease inherent aberrations in electron lenses by employing multi-pole correctors [6]. Other methods may surpass the resolution of the lens, irrespective of aberrations or partial coherence via ptychography [7] or Wigner distribution deconvolution [8]. Hence, it may be timely to consider the usefulness of information about 2D projections of 3D amorphous materials.

† Present address: School of Physical Sciences, University of Kent, Canterbury CT2 7NR, UK.

0953-8984/99/112319+18$19.50

Interpretation of the projection of an amorphous structure is problematic because amorphous solids contain overlapping, disordered layers of atoms [9, 10]. This characteristic would remain even if resolution were to be improved to the point where images are 'perfect'. Previously, workers have considered special cases, such as when the sample contains only a few layers of atoms [11] (although such samples cannot feasibly be prepared [12]), or when there is medium range order within regions of the sample, such as crystallites [13] or quasi-Bragg planes [14].

In this paper, we consider the general case of thin amorphous (3D) structures and identify structural information present in their 2D projections [15]. Our approach is to use distribution functions which describe the degree of order in a structure. We use a particular set of distribution functions which have quite general definitions [16]. This set includes the pair distribution function (PDF), which is the most commonly used function for describing amorphous structures, because it can be measured in a diffraction experiment [16]. Also included is the triplet distribution function (TDF) which has been shown to influence the structural signal in extended x-ray absorption fine structure experiments [17]. Note, however, that these are not the only existing functions for describing the degree of order in disordered structures (e.g. bond orientational order functions [18]).

2. Theory

2.1. Distribution functions for 3D structures

The problem of describing order in disordered structures has been approached by using distribution functions. We begin by reviewing a set of distribution functions for describing 3D structures [16]. A 3D structure of N particles with positions $\boldsymbol{R}_\ell$ is described by the single particle density function,

$$\rho(\boldsymbol{r}) = \sum_\ell \delta(\boldsymbol{r} - \boldsymbol{R}_\ell)$$

(there are no assumptions about particle positions). This has the property

$$\int \rho(\boldsymbol{r})\,\mathrm{d}\boldsymbol{r} = N.$$

The average of this function over arbitrary origins is the atomic density,

$$\rho_0 = \frac{1}{V}\int \rho(\boldsymbol{r}+\boldsymbol{r}')\,\mathrm{d}\boldsymbol{r}' = \frac{1}{V}\int \rho(\boldsymbol{r}'')\,\mathrm{d}\boldsymbol{r}'' = N/V.$$

The correlations between pairs of atoms are described by the two particle density function,

$$\rho 2(\boldsymbol{r}_1,\boldsymbol{r}_2) = \sum_\ell \delta(\boldsymbol{r}_1 - \boldsymbol{R}_\ell)\left(\sum_m \delta(\boldsymbol{r}_2 - \boldsymbol{R}_m) - \delta(\boldsymbol{r}_1 - \boldsymbol{r}_2)\right)$$

which excludes the case of $\boldsymbol{r}_1 = \boldsymbol{r}_2$. This function has the properties

$$\int \rho 2(\boldsymbol{r}_1,\boldsymbol{r}_2)\,\mathrm{d}\boldsymbol{r}_2 = (N-1)\sum_\ell \delta(\boldsymbol{r}_1 - \boldsymbol{R}_\ell) = (N-1)\rho(\boldsymbol{r}_1)$$

and

$$\begin{aligned}\rho 2(\boldsymbol{r}_1,\boldsymbol{r}_2) &= \sum_\ell\sum_m \delta(\boldsymbol{r}_1 - \boldsymbol{R}_\ell)\delta(\boldsymbol{r}_2 - \boldsymbol{R}_m) - \sum_\ell \delta(\boldsymbol{r}_1 - \boldsymbol{R}_\ell)\delta(\boldsymbol{r}_1 - \boldsymbol{r}_2)\\ &= \sum_m\sum_\ell \delta(\boldsymbol{r}_2 - \boldsymbol{R}_m)\delta(\boldsymbol{r}_1 - \boldsymbol{R}_\ell) - \sum_m \delta(\boldsymbol{r}_2 - \boldsymbol{R}_m)\delta(\boldsymbol{r}_1 - \boldsymbol{r}_2) = \rho 2(\boldsymbol{r}_2,\boldsymbol{r}_1).\end{aligned}$$

The average of this function over arbitrary origins,

$$\begin{aligned}\rho 2(\boldsymbol{r}_{12}) &= \frac{1}{V}\int \rho 2(\boldsymbol{r}_1+\boldsymbol{r}', \boldsymbol{r}_2+\boldsymbol{r}')\,\mathrm{d}\boldsymbol{r} = \frac{1}{V}\int \rho 2(\boldsymbol{r}'', \boldsymbol{r}_{12}+\boldsymbol{r}'')\,\mathrm{d}\boldsymbol{r}'' \\ &= \frac{1}{V}\int \sum_\ell \delta(\boldsymbol{r}''-\boldsymbol{R}_\ell)\Big(\sum_m \delta(\boldsymbol{r}_{12}+\boldsymbol{r}''-\boldsymbol{R}_m)-\delta(\boldsymbol{r}_{12})\Big)\,\mathrm{d}\boldsymbol{r}'' \\ &= \frac{1}{V}\sum_\ell\Big(\sum_m \delta(\boldsymbol{r}_{12}-(\boldsymbol{R}_m-\boldsymbol{R}_\ell))-\delta(\boldsymbol{r}_{12})\Big) \qquad (1)\end{aligned}$$

depends only on a single vector $\boldsymbol{r}_{12}=\boldsymbol{r}_2-\boldsymbol{r}_1$ which represents the possible separations of pairs of atoms. This function is related to the autocorrelation function [16],

$$\begin{aligned}\int \rho(\boldsymbol{r}')\rho(\boldsymbol{r}_{12}+\boldsymbol{r}')\,\mathrm{d}\boldsymbol{r}' &= \int \sum_\ell \delta(\boldsymbol{r}'-\boldsymbol{R}_\ell)\sum_m \delta(\boldsymbol{r}_{12}+\boldsymbol{r}'-\boldsymbol{R}_m)\,\mathrm{d}\boldsymbol{r}' \\ &= \int \sum_\ell \delta(\boldsymbol{r}'-\boldsymbol{R}_\ell)\Big(\sum_m \delta(\boldsymbol{r}_{12}+\boldsymbol{r}'-\boldsymbol{R}_m)-\delta(\boldsymbol{r}_{12})\Big)\,\mathrm{d}\boldsymbol{r}' \\ &\quad + \int \sum_\ell \delta(\boldsymbol{r}'-\boldsymbol{R}_\ell)\delta(\boldsymbol{r}_{12})\,\mathrm{d}\boldsymbol{r}' = V\rho 2(\boldsymbol{r}_{12})+N\delta(\boldsymbol{r}_{12})\end{aligned}$$

which includes the case of $\boldsymbol{r}_1=\boldsymbol{r}_2$. For comparison of structures with different densities, it is useful to use the pair distribution function (PDF),

$$g(\boldsymbol{r}_{12}) = \rho 2(\boldsymbol{r}_{12})/\rho_0^2. \qquad (2)$$

This function gives the frequencies of different interatomic distances relative to those expected for a totally random structure, i.e. with a random set of positions $\boldsymbol{R}_i$, which would have $g(\boldsymbol{r}_{12})=1$. For isotropic structures it is useful to consider the radial average of $g(\boldsymbol{r}_{12})$,

$$g(r_{12}) = \frac{1}{4\pi r_{12}^2}\iint g(\boldsymbol{r}_{12})r_{12}^2\sin(\theta_{12})\,\mathrm{d}\varphi_{12}\,\mathrm{d}\theta_{12} \qquad (3)$$

which depends only on $r_{12}=|\boldsymbol{r}_{12}|$.

It is possible to describe higher order correlations. Here we will specifically consider correlations between triplets of atoms. These are described by the three particle density function,

$$\begin{aligned}\rho 3(\boldsymbol{r}_1,\boldsymbol{r}_2,\boldsymbol{r}_3) &= \sum_\ell \delta(\boldsymbol{r}_1-\boldsymbol{R}_\ell)\Big(\sum_m \delta(\boldsymbol{r}_2-\boldsymbol{R}_m)-\delta(\boldsymbol{r}_2-\boldsymbol{r}_1)\Big) \\ &\quad\times\Big(\sum_n \delta(\boldsymbol{r}_3-\boldsymbol{R}_n)-\delta(\boldsymbol{r}_3-\boldsymbol{r}_1)-\delta(\boldsymbol{r}_3-\boldsymbol{r}_2)\Big)\end{aligned}$$

which excludes the cases of $\boldsymbol{r}_1=\boldsymbol{r}_2$, $\boldsymbol{r}_1=\boldsymbol{r}_3$, $\boldsymbol{r}_2=\boldsymbol{r}_3$ or $\boldsymbol{r}_1=\boldsymbol{r}_2=\boldsymbol{r}_3$. This function has the properties

$$\begin{aligned}\int \rho 3(\boldsymbol{r}_1,\boldsymbol{r}_2,\boldsymbol{r}_3)\,\mathrm{d}\boldsymbol{r}_3 &= (N-2)\sum_\ell \delta(\boldsymbol{r}_1-\boldsymbol{R}_\ell)\Big(\sum_m \delta(\boldsymbol{r}_2-\boldsymbol{R}_m)-\delta(\boldsymbol{r}_2-\boldsymbol{r}_1)\Big) \\ &= (N-2)\rho 2(\boldsymbol{r}_1,\boldsymbol{r}_2) \\ \rho 3(\boldsymbol{r}_1,\boldsymbol{r}_2,\boldsymbol{r}_3) &= \sum_\ell\Big(\sum_m \delta(\boldsymbol{r}_1-\boldsymbol{R}_\ell)\delta(\boldsymbol{r}_2-\boldsymbol{R}_m)-\delta(\boldsymbol{r}_1-\boldsymbol{R}_\ell)\delta(\boldsymbol{r}_2-\boldsymbol{r}_1)\Big) \\ &\quad\times\Big(\sum_n \delta(\boldsymbol{r}_3-\boldsymbol{R}_n)-\delta(\boldsymbol{r}_3-\boldsymbol{r}_1)-\delta(\boldsymbol{r}_3-\boldsymbol{r}_2)\Big)\end{aligned}$$

$$= \sum_m \left(\sum_\ell \delta(\boldsymbol{r}_2 - \boldsymbol{R}_m)\delta(\boldsymbol{r}_1 - \boldsymbol{R}_\ell) - \delta(\boldsymbol{r}_2 - \boldsymbol{R}_m)\delta(\boldsymbol{r}_2 - \boldsymbol{r}_1) \right)$$
$$\times \left(\sum_n \delta(\boldsymbol{r}_3 - \boldsymbol{R}_n) - \delta(\boldsymbol{r}_3 - \boldsymbol{r}_2) - \delta(\boldsymbol{r}_3 - \boldsymbol{r}_1) \right) = \rho 3(\boldsymbol{r}_2, \boldsymbol{r}_1, \boldsymbol{r}_3)$$

and

$$\rho 3(\boldsymbol{r}_1, \boldsymbol{r}_2, \boldsymbol{r}_3) = \sum_\ell \delta(\boldsymbol{r}_1 - \boldsymbol{R}_\ell) \left(\sum_m \delta(\boldsymbol{r}_2 - \boldsymbol{R}_m) \sum_n \delta(\boldsymbol{r}_3 - \boldsymbol{R}_n) \right.$$
$$- \sum_m \delta(\boldsymbol{r}_2 - \boldsymbol{R}_m)\delta(\boldsymbol{r}_3 - \boldsymbol{r}_1) - \sum_m \delta(\boldsymbol{r}_2 - \boldsymbol{R}_m)\delta(\boldsymbol{r}_3 - \boldsymbol{r}_2)$$
$$\left. -\delta(\boldsymbol{r}_2 - \boldsymbol{r}_1) \sum_n \delta(\boldsymbol{r}_3 - \boldsymbol{R}_n) + \delta(\boldsymbol{r}_2 - \boldsymbol{r}_1)\delta(\boldsymbol{r}_3 - \boldsymbol{r}_1) + \delta(\boldsymbol{r}_2 - \boldsymbol{r}_1)\delta(\boldsymbol{r}_3 - \boldsymbol{r}_2) \right)$$
$$= \sum_\ell \delta(\boldsymbol{r}_1 - \boldsymbol{R}_\ell) \left(\sum_n (\delta(\boldsymbol{r}_3 - \boldsymbol{R}_n) \sum_m (\boldsymbol{r}_2 - \boldsymbol{R}_m) \right.$$
$$-\delta(\boldsymbol{r}_3 - \boldsymbol{r}_1) \sum_m \delta(\boldsymbol{r}_2 - \boldsymbol{R}_m) - \sum_n \delta(\boldsymbol{r}_3 - \boldsymbol{R}_n)\delta(\boldsymbol{r}_2 - \boldsymbol{r}_3)$$
$$- \sum_n \delta(\boldsymbol{r}_3 - \boldsymbol{R}_n)\delta(\boldsymbol{r}_2 - \boldsymbol{r}_1) + \delta(\boldsymbol{r}_3 - \boldsymbol{r}_1)\delta(\boldsymbol{r}_2 - \boldsymbol{r}_1)$$
$$\left. +\delta(\boldsymbol{r}_3 - \boldsymbol{r}_1)\delta(\boldsymbol{r}_2 - \boldsymbol{r}_3) \right) = \rho 3(\boldsymbol{r}_1, \boldsymbol{r}_3, \boldsymbol{r}_2).$$

The average of this function for arbitrary origins,

$$\rho 3(\boldsymbol{r}_{12}, \boldsymbol{r}_{13}) = \frac{1}{V} \int \rho 3(\boldsymbol{r}_1 + \boldsymbol{r}', \boldsymbol{r}_2 + \boldsymbol{r}', \boldsymbol{r}_3 + \boldsymbol{r}')\, \mathrm{d}\boldsymbol{r}' = \frac{1}{V} \int \rho 3(\boldsymbol{r}'', \boldsymbol{r}_{12} + \boldsymbol{r}'', \boldsymbol{r}_{13} + \boldsymbol{r}'')\, \mathrm{d}\boldsymbol{r}''$$
$$= \frac{1}{V} \int \sum_\ell \delta(\boldsymbol{r}'' - \boldsymbol{R}_\ell) \left(\sum_m \delta(\boldsymbol{r}_{12} + \boldsymbol{r}'' - \boldsymbol{R}_m) - \delta(\boldsymbol{r}_{12}) \right)$$
$$\times \left(\sum_n \delta(\boldsymbol{r}_{13} + \boldsymbol{r}'' - \boldsymbol{R}_n) - \delta(\boldsymbol{r}_{13}) - \delta(\boldsymbol{r}_{13} - \boldsymbol{r}_{12}) \right) \mathrm{d}\boldsymbol{r}''$$
$$= \frac{1}{V} \sum_\ell \left(\sum_m \delta(\boldsymbol{r}_{12} - (\boldsymbol{R}_m - \boldsymbol{R}_\ell)) - \delta(\boldsymbol{r}_{12}) \right)$$
$$\times \left(\sum_n \delta(\boldsymbol{r}_{13} - (\boldsymbol{R}_n - \boldsymbol{R}_\ell) - \delta(\boldsymbol{r}_{13}) - \delta(\boldsymbol{r}_{13} - \boldsymbol{r}_{12}) \right) \tag{4}$$

depends only on $\boldsymbol{r}_{12} = \boldsymbol{r}_2 - \boldsymbol{r}_1$ and $\boldsymbol{r}_{13} = \boldsymbol{r}_3 - \boldsymbol{r}_1$ (i.e. six dimensions) which describe the possible separations of triplets of atoms. This function is related to the triple autocorrelation function [19],

$$\int \rho(\boldsymbol{r}')\rho(\boldsymbol{r}_{12} + \boldsymbol{r}')\rho(\boldsymbol{r}_{13} + \boldsymbol{r}')\, \mathrm{d}\boldsymbol{r}'$$
$$= \int \sum_\ell \delta(\boldsymbol{r}' - \boldsymbol{R}_\ell) \sum_m \delta(\boldsymbol{r}_{12} + \boldsymbol{r}' - \boldsymbol{R}_m) \sum_n \delta(\boldsymbol{r}_{13} + \boldsymbol{r}' - \boldsymbol{R}_n)\, \mathrm{d}\boldsymbol{r}'$$
$$= \int \sum_\ell \delta(\boldsymbol{r}' - \boldsymbol{R}_\ell) \left(\sum_m \delta(\boldsymbol{r}_{12} + \boldsymbol{r}' - \boldsymbol{R}_m) - \delta(\boldsymbol{r}_{12}) \right)$$
$$\times \left(\sum_n \delta(\boldsymbol{r}_{13} + \boldsymbol{r}' - \boldsymbol{R}_n) - \delta(\boldsymbol{r}_{13}) - \delta(\boldsymbol{r}_{13} - \boldsymbol{r}_{12}) \right) \mathrm{d}\boldsymbol{r}'$$

$$
\begin{aligned}
&+\int \sum_{\ell} \delta(\boldsymbol{r}' - \boldsymbol{R}_\ell) \sum_{m} \delta(\boldsymbol{r}_{12} + \boldsymbol{r}' - \boldsymbol{R}_m)(\delta(\boldsymbol{r}_{13}) + \delta(\boldsymbol{r}_{13} - \boldsymbol{r}_{12}))\,\mathrm{d}\boldsymbol{r}' \\
&+\int \Bigg(\sum_{\ell} \delta(\boldsymbol{r}' - \boldsymbol{R}_\ell)\delta(\boldsymbol{r}_{12}) \sum_{n} \delta(\boldsymbol{r}_{13} + \boldsymbol{r}' - \boldsymbol{R}_n) \\
&-\sum_{\ell} \delta(\boldsymbol{r}' - \boldsymbol{R}_\ell)\delta(\boldsymbol{r}_{12})(\delta(\boldsymbol{r}_{13}) + \delta(\boldsymbol{r}_{13} - \boldsymbol{r}_{12}))\Bigg)\,\mathrm{d}\boldsymbol{r}' \\
&= V\rho 3(\boldsymbol{r}_{12}, \boldsymbol{r}_{13}) + V(\rho 2(\boldsymbol{r}_{12})\delta(\boldsymbol{r}_{13}) + \rho 2(\boldsymbol{r}_{12})\delta(\boldsymbol{r}_{13} - \boldsymbol{r}_{12}) \\
&\quad +\rho 2(\boldsymbol{r}_{13})\delta(\boldsymbol{r}_{12})) + N\delta(\boldsymbol{r}_{12})\delta(\boldsymbol{r}_{13})
\end{aligned}
$$

which includes the cases of $\boldsymbol{r}_1 = \boldsymbol{r}_2$, $\boldsymbol{r}_1 = \boldsymbol{r}_3$, $\boldsymbol{r}_2 = \boldsymbol{r}_3$ and $\boldsymbol{r}_1 = \boldsymbol{r}_2 = \boldsymbol{r}_3$. For comparison of structures with different densities, it is useful to use the triplet distribution function (TDF),

$$g3(\boldsymbol{r}_{12}, \boldsymbol{r}_{13}) = \rho 3(\boldsymbol{r}_{12}, \boldsymbol{r}_{13})/\rho_0^3. \tag{5}$$

This function gives the frequencies of different arrangements of triplets of atoms relative to those expected for a totally random structure, i.e. with a random set of positions $\boldsymbol{R}_i$, which would have $g3(\boldsymbol{r}_{12}, \boldsymbol{r}_{23}) = 1$. For isotropic structures it is useful to consider the orientational average of $g3(\boldsymbol{r}_{12}, \boldsymbol{r}_{23})$,

$$g3(r_{12}, r_{13}, \theta_{23}) = \frac{1}{4\pi r_{12}^2 2\pi r_{13}} \int\int\int g3(\boldsymbol{r}_{12}, \boldsymbol{r}_{13}) r_{12}^2 \sin(\theta_{12})\,\mathrm{d}\varphi_{12}\,\mathrm{d}\theta_{12} r_{13} \sin(\theta_{23})\,\mathrm{d}\varphi_{23} \tag{6}$$

which depends only on $r_{12} = |\boldsymbol{r}_{12}|$ and $\boldsymbol{r}_{13} = |\boldsymbol{r}_{13}|$, and θ_{23}, the angle between $\boldsymbol{r}_{12}$ and $\boldsymbol{r}_{13}$.

2.2. Distribution functions for 2D structures

It is possible to define analogous functions for 2D structures, and we denote these functions using the subscript '2D'. The notation $\tilde{\boldsymbol{r}}$ identifies 2D vectors (x, y). There are changes in the dependent variables and limits of integration, and in the normalization constants for isotropic averaging, relative to those for 3D structures. For an isotropic 2D structure, the radial averages of the PDF and TDF (respectively) are

$$g_{2D}(\tilde{r}_{12}) = \frac{1}{2\pi \tilde{r}_{12}} \int g_{2D}(\tilde{\boldsymbol{r}}_{12}) \tilde{r}_{12}\,\mathrm{d}\phi_{12} \tag{7}$$

and

$$g3_{2D}(\tilde{r}_{12}, \tilde{r}_{13}, \phi_{23}) = \frac{1}{4\pi \tilde{r}_{12}} \int g3_{2D}(\tilde{\boldsymbol{r}}_{12}, \tilde{\boldsymbol{r}}_{13}) \tilde{r}_{12}\,\mathrm{d}\phi_{12}. \tag{8}$$

The latter normalization includes a factor of 2 because ϕ_{23}, the angle between $\tilde{\boldsymbol{r}}_{12}$ and $\tilde{\boldsymbol{r}}_{13}$, is restricted to lie in the range 0 to π.

2.3. Pair distribution functions for 2D projections

We now consider the special case of a 2D structure which is the 2D projection of a 3D structure. The appropriate functions are the same as those for a 2D structure, but we denote these functions using the subscript P for the special case of a 2D projection. For simplicity we assume a structure with boundaries parallel to the (x, y) plane and thickness t in the z direction, i.e. $0 \leqslant z \leqslant t$. Here we are concerned with the relationship of these functions to those describing the 3D structure from which the 2D projection is generated. The relationship between the one particle density functions is

$$\rho_P(\tilde{\boldsymbol{r}}) = \sum_{\ell} \delta(\tilde{\boldsymbol{r}} - (X, Y)_\ell) = \int_0^t \sum_{\ell} \delta(\boldsymbol{r} - \boldsymbol{R}_\ell)\,\mathrm{d}z = \int_0^t \rho(\boldsymbol{r})\,\mathrm{d}z.$$

The relationship between the averages of these functions for different origins is

$$\rho_{0P} = \frac{1}{A}\int \rho(\tilde{\boldsymbol{r}} + \tilde{\boldsymbol{r}}')\,\mathrm{d}\tilde{\boldsymbol{r}}' = \frac{t}{V}\int\int_0^t \rho(\boldsymbol{r} + \tilde{\boldsymbol{r}}')\,\mathrm{d}z\,\mathrm{d}\tilde{\boldsymbol{r}}' = \frac{t}{V}\int\int_0^t \rho(\boldsymbol{r}'')\,\mathrm{d}z''\,\mathrm{d}\tilde{\boldsymbol{r}}'' = t\rho_0$$

where $z'' = z$ and $\tilde{\boldsymbol{r}}'' = \tilde{\boldsymbol{r}}_1 + \tilde{\boldsymbol{r}}'$. The relationships between the two particle density functions are

$$\begin{aligned}\rho 2_P(\tilde{\boldsymbol{r}}_1, \tilde{\boldsymbol{r}}_2) &= \sum_\ell \delta(\tilde{\boldsymbol{r}}_1 - (X, Y)_\ell)\left(\sum_m \delta(\tilde{\boldsymbol{r}}_2 - (X, Y)_m)) - \delta(\tilde{\boldsymbol{r}}_2 - \tilde{\boldsymbol{r}}_1)\right)\\ &= \int_0^t\int_0^t \sum_\ell \delta(\boldsymbol{r}_1 - \boldsymbol{R}_\ell)\left(\sum_m \delta(\boldsymbol{r}_2 - \boldsymbol{R}_m) - \delta(\boldsymbol{r}_1 - \boldsymbol{r}_2)\right)\mathrm{d}z_1\,\mathrm{d}z_2\\ &= \int_0^t\int_0^t \rho 2(\boldsymbol{r}_1, \boldsymbol{r}_2)\,\mathrm{d}z_2\,\mathrm{d}z_2\end{aligned}$$

and

$$\rho 2_P(\tilde{\boldsymbol{r}}_{12}) = \frac{1}{A}\int \rho 2_P(\tilde{\boldsymbol{r}}_1 + \tilde{\boldsymbol{r}}', \tilde{\boldsymbol{r}}_2 + \tilde{\boldsymbol{r}}')\,\mathrm{d}\tilde{\boldsymbol{r}}' = \frac{t}{V}\int\int_0^t\int_0^t \rho 2(\boldsymbol{r}_1 + \tilde{\boldsymbol{r}}', \boldsymbol{r}_2 + \tilde{\boldsymbol{r}}')\,\mathrm{d}z_1\,\mathrm{d}z_2\,\mathrm{d}\tilde{\boldsymbol{r}}'.$$

The integrals over z_1 and z_2 can be rearranged by changing the variables of integration to $z'' = z_1$ and $z_{12} = z_2 - z_1$, in the following manner:

$$\int_0^t\int_0^t \ldots\,\mathrm{d}z_1\,\mathrm{d}z_2 = \int_{-t}^0\int_{-z_{12}}^t \ldots\,\mathrm{d}z''\,\mathrm{d}z_{12} + \int_0^t\int_0^{t-z_{12}} \ldots\,\mathrm{d}z''\,\mathrm{d}z_{12}.$$

Using $\mathrm{d}\tilde{\boldsymbol{r}}'' = \mathrm{d}\tilde{\boldsymbol{r}}' + \mathrm{d}\tilde{\boldsymbol{r}}_1$, the expression for $\rho 2_P(\tilde{\boldsymbol{r}}_{12})$ becomes

$$\begin{aligned}\rho 2_P(\tilde{\boldsymbol{r}}_{12}) = t\int_{-t}^0 \left(\frac{1}{V}\int\int_{-z_{12}}^t \rho 2(\boldsymbol{r}'', \boldsymbol{r}_{12} + \boldsymbol{r}'')\,\mathrm{d}z''\,\mathrm{d}\tilde{\boldsymbol{r}}''\right)\mathrm{d}z_{12}\\ + t\int_0^t \left(\frac{1}{V}\int\int_0^{t-z_{12}} \rho 2(\boldsymbol{r}'', \boldsymbol{r}_{12} + \boldsymbol{r}'')\,\mathrm{d}z''\,\mathrm{d}\tilde{\boldsymbol{r}}''\right)\mathrm{d}z_{12}. \qquad (9)\end{aligned}$$

The bracketed expression in equation (9) is equal to $\rho 2_{thin}(\boldsymbol{r}_{12})$, the average over arbitrary origins of $\rho 2(\boldsymbol{r}'', \boldsymbol{r}_{12} + \boldsymbol{r}'')$ for the 3D structure from which the 2D projection is derived. This is because $\rho 2(\boldsymbol{r}'', \boldsymbol{r}_{12} + \boldsymbol{r}'')$ is zero outside the limits of the integral for z'', which can thus be extended to include all arbitrary origins.

However, studies of amorphous structures are usually concerned with 3D structures with effectively infinite thickness. This is because the pair distribution functions are measured using diffraction on samples with dimensions typically 10^6 greater than interatomic distances, or they are calculated from models which have periodic boundary conditions. Hence it is most useful to reformulate the integral in equation (9) in terms of a bulk 3D structure, i.e. with $\rho 2_{bulk}(\boldsymbol{r}_{12})$. To do this, it is necessary to explicitly represent the effects of finite thickness. From the limits of integration in equation (9), it can be seen that the appropriate factor is $(1 - |z_{12}|/t)$. Hence

$$\rho 2_P(\tilde{\boldsymbol{r}}_{12}) = t\int_{-t}^t \left(1 - \frac{|z_{12}|}{t}\right)\rho 2_{bulk}(\boldsymbol{r}_{12})\,\mathrm{d}z_{12}.$$

The accuracy of this reformulation depends on the following approximations, which are reasonable for a homogenous, amorphous structure:

$$\int_0^a \rho 2(\boldsymbol{r}'', \boldsymbol{r}_{12} + \boldsymbol{r}'')\,\mathrm{d}z'' = \int_b^{a+b} \rho 2(\boldsymbol{r}'', \boldsymbol{r}_{12} + \boldsymbol{r}'')\,\mathrm{d}z''$$

and

$$\int_0^a \rho 2(\boldsymbol{r}'', \boldsymbol{r}_{12} + \boldsymbol{r}'')\,\mathrm{d}z'' = \frac{a}{b}\int_0^b \rho 2(\boldsymbol{r}'', \boldsymbol{r}_{12} + \boldsymbol{r}'')\,\mathrm{d}z''.$$

Then the relationship between the PDFs is

$$g_P(\tilde{\boldsymbol{r}}_{12}) = \frac{1}{t}\int_{-t}^{t}\left(1-\frac{|z_{12}|}{t}\right)g(\boldsymbol{r}_{12})\,\mathrm{d}z_{12}$$

where a t^{-2} factor comes from the difference between ρ_0^2 and ρ_{0P}^2. The relationship between the isotropic PDFs,

$$g_P(\tilde{r}_{12}) = \frac{1}{t}\int_{-t}^{t}\left(1-\frac{|z_{12}|}{t}\right)g((\tilde{r}_{12}^2+z_{12}^2)^{0.5})\,\mathrm{d}z_{12} \tag{10}$$

depends on t and the projected interatomic distance $\tilde{r}_{12}$.

2.4. Triplet distribution functions for 2D projections

The relationships between the three particle density functions are

$$\begin{aligned}
\rho 3_P(\tilde{\boldsymbol{r}}_1,\tilde{\boldsymbol{r}}_2,\tilde{\boldsymbol{r}}_3) &= \sum_\ell \delta(\tilde{\boldsymbol{r}}_1-(X,Y)_\ell)\left(\sum_m \delta(\tilde{\boldsymbol{r}}_2-(X,Y)_m)-\delta(\tilde{\boldsymbol{r}}_1-\tilde{\boldsymbol{r}}_2)\right)\\
&\quad\times\left(\sum_n \delta(\tilde{\boldsymbol{r}}_3-(X,Y)_n)-\delta(\tilde{\boldsymbol{r}}_3-\tilde{\boldsymbol{r}}_1)-\delta(\tilde{\boldsymbol{r}}_3-\tilde{\boldsymbol{r}}_2)\right)\\
&= \int_0^t\int_0^t\int_0^t \sum_\ell \delta(\boldsymbol{r}_1-\boldsymbol{R}_\ell)\left(\sum_m \delta(\boldsymbol{r}_2-\boldsymbol{R}_m)-\delta(\boldsymbol{r}_1-\boldsymbol{r}_2)\right)\\
&\quad\times\left(\sum_n \delta(\boldsymbol{r}_3-\boldsymbol{R}_n)-\delta(\boldsymbol{r}_3-\boldsymbol{r}_1)-\delta(\boldsymbol{r}_3-\boldsymbol{r}_2)\right)\mathrm{d}z_1\,\mathrm{d}z_2\,\mathrm{d}z_3\\
&= \int_0^t\int_0^t\int_0^t \rho 3(\boldsymbol{r}_1,\boldsymbol{r}_2,\boldsymbol{r}_3)\,\mathrm{d}z_1\,\mathrm{d}z_2\,\mathrm{d}z_3
\end{aligned}$$

and

$$\begin{aligned}
\rho 3_P(\tilde{\boldsymbol{r}}_{12},\tilde{\boldsymbol{r}}_{13}) &= \frac{1}{A}\int \rho 3_P(\tilde{\boldsymbol{r}}_1+\tilde{\boldsymbol{r}}',\tilde{\boldsymbol{r}}_2+\tilde{\boldsymbol{r}}',\tilde{\boldsymbol{r}}_3+\tilde{\boldsymbol{r}}')\,\mathrm{d}\tilde{\boldsymbol{r}}'\\
&= \frac{t}{V}\int\int_0^t\int_0^t\int_0^t \rho 3(\boldsymbol{r}_1+\tilde{\boldsymbol{r}}',\boldsymbol{r}_2+\tilde{\boldsymbol{r}}',\boldsymbol{r}_3+\tilde{\boldsymbol{r}}')\,\mathrm{d}z_1\,\mathrm{d}z_2\,\mathrm{d}z_3\,\mathrm{d}\tilde{\boldsymbol{r}}'.
\end{aligned}$$

The integrals over z_1, z_2 and z_3 can be rearranged by changing the variables of integration to $z''=z_1$, $z_{12}=z_2-z_1$ and $z_{13}=z_3-z_1$, in the following manner:

$$\begin{aligned}
\frac{t}{V}\int_0^t\int_0^t\int_0^t \ldots\,\mathrm{d}z_1\,\mathrm{d}z_2\,\mathrm{d}z_3 &= t\int_{-t}^{0}\int_{-t}^{z_{13}}\left(\frac{1}{V}\int_{-z_{12}}^{t}\ldots\,\mathrm{d}z''\right)\mathrm{d}z_{12}\,\mathrm{d}z_{13}\\
&\quad+t\int_0^t\int_{z_{13}}^{t}\left(\frac{1}{V}\int_0^{t-z_{12}}\ldots\,\mathrm{d}z''\right)\mathrm{d}z_{12}\,\mathrm{d}z_{13}\\
&\quad+t\int_{-t}^{0}\int_0^{t+z_{13}}\left(\frac{1}{V}\int_{-z_{13}}^{t-z_{12}}\ldots\,\mathrm{d}z''\right)\mathrm{d}z_{12}\,\mathrm{d}z_{13}\\
&\quad+t\int_0^t\int_{z_{13-t}}^{0}\left(\frac{1}{V}\int_{-z_{12}}^{t-z_{13}}\ldots\,\mathrm{d}z''\right)\mathrm{d}z_{12}\,\mathrm{d}z_{13}\\
&\quad+t\int_{-t}^{0}\int_{-t}^{z_{12}}\left(\frac{1}{V}\int_{-z_{13}}^{t}\ldots\,\mathrm{d}z''\right)\mathrm{d}z_{13}\,\mathrm{d}z_{12}\\
&\quad+t\int_0^t\int_{z_{12}}^{t}\left(\frac{1}{V}\int_0^{t-z_{13}}\ldots\,\mathrm{d}z''\right)\mathrm{d}z_{13}\,\mathrm{d}z_{12}.
\end{aligned} \tag{11}$$

The central integral in equation (11) is equal to $\rho 3_{thin}(\boldsymbol{r}_{12}, \boldsymbol{r}_{13})$, the average over arbitrary origins of $\rho 3(\boldsymbol{r}_1 + \boldsymbol{r}'', \boldsymbol{r}_2 + \boldsymbol{r}'', \boldsymbol{r}_3 + \boldsymbol{r}'')$ for the 3D structure from which the 2D projection is derived (using $\mathrm{d}\boldsymbol{r}'' = \mathrm{d}z''\,\mathrm{d}\tilde{\boldsymbol{r}}''$, where $\mathrm{d}\tilde{\boldsymbol{r}}'' = \mathrm{d}\tilde{\boldsymbol{r}}' + \mathrm{d}\tilde{\boldsymbol{r}}_1$). This is because $\rho 3(\boldsymbol{r}_1 + \boldsymbol{r}'', \boldsymbol{r}_2 + \boldsymbol{r}'', \boldsymbol{r}_3 + \boldsymbol{r}'')$ is zero outside the limits of the integral for z'', which can thus be extended to include all arbitrary origins.

However, studies of amorphous structures are usually concerned with 3D structures with effectively infinite thickness, as discussed in the previous section. Hence it is most useful to reformulate the integral in equation (11) in terms of a bulk 3D structure, i.e. with the function $\rho 3_{bulk}(\boldsymbol{r}_{12}, \boldsymbol{r}_{13})$. To do this, it is necessary to explicitly represent the effects of finite thickness. This involves equivalent assumptions to those used in the previous section (which are reasonable for homogeneous, amorphous structures), but the resulting expression,

$$\begin{aligned}\rho 3_P(\tilde{\boldsymbol{r}}_{12}, \tilde{\boldsymbol{r}}_{13}) = {} & t\int_{-t}^{0}\int_{-t}^{0}\left(1+\frac{z_{12}}{t}\right)\left(1+\frac{z_{13}}{t}\right)\rho 3_{bulk}(\boldsymbol{r}_{12}, \boldsymbol{r}_{13})\,\mathrm{d}z_{12}\,\mathrm{d}z_{13} \\ & + t\int_{0}^{t}\int_{0}^{t}\left(1-\frac{z_{12}}{t}\right)\left(1-\frac{z_{13}}{t}\right)\rho 3_{bulk}(\boldsymbol{r}_{12}, \boldsymbol{r}_{13})\,\mathrm{d}z_{12}\,\mathrm{d}z_{13} \\ & + t\int_{-t}^{0}\int_{0}^{t-z_{13}}\left(1+\frac{(z_{13}-z_{12})}{t}\right)\rho 3_{bulk}(\boldsymbol{r}_{12}, \boldsymbol{r}_{13})\,\mathrm{d}z_{12}\,\mathrm{d}z_{13} \\ & + t\int_{0}^{t}\int_{z_{13}-t}^{0}\left(1-\frac{(z_{13}-z_{12})}{t}\right)\rho 3_{bulk}(\boldsymbol{r}_{12}, \boldsymbol{r}_{13})\,\mathrm{d}z_{12}\,\mathrm{d}z_{13}\end{aligned}$$

is more complex. In particular, the integral over z_{12} and z_{13} is restricted, due to the requirement that $-t \leqslant (z_{13} - z_{12}) \leqslant t$. For clarity, we represent the integral in schematic form in the following. Then the relationship between the TDFs is

$$g3_p(\tilde{\boldsymbol{r}}_{12}, \tilde{\boldsymbol{r}}_{13}) \approx \frac{1}{t^2}\int_{-t}^{t}\int_{-t}^{t}\left(1 \pm \frac{z_{12}}{t}\right)\left(1 \pm \frac{z_{13}}{t}\right) g3(\boldsymbol{r}_{12}, \boldsymbol{r}_{13})\,\mathrm{d}z_{12}\,\mathrm{d}z_{13}$$

where a t^{-3} factor comes from the difference between ρ_0^3 and ρ_{0P}^3. The relationship between the isotropic TDFs,

$$\begin{aligned}& g3_P(\tilde{r}_{12}, \tilde{r}_{13}, \phi_{23}) \\ & \quad \approx \int_{-t}^{t}\int_{-t}^{t}\left(1 \pm \frac{z_{12}}{t}\right)\left(1 \pm \frac{z_{13}}{t}\right) g_3((\tilde{r}_{12}^2 + z_{12}^2)^{0.5}, (\tilde{r}_{13}^2 + z_{13}^2)^{0.5}, \theta_{23})\,\mathrm{d}z_{12}\,\mathrm{d}z_{13}\end{aligned} \tag{12}$$

depends on t, the projected interatomic distances $\tilde{r}_{12}$ and $\tilde{r}_{13}$ and the projected angle between them, ϕ_{23}, where

$$\cos(\theta_{23}) = \frac{\tilde{r}_{12}\tilde{r}_{13}\cos(\phi_{23}) + z_{12}z_{13}}{(\tilde{r}_{12}^2 + z_{12}^2)^{0.5}(\tilde{r}_{13}^2 + z_{13}^2)^{0.5}}$$

(using the cosine rule). Figure 1 illustrates the relationship between the dependent variables in the 3D structure and the 2D projection.

2.5. Analytical expressions for the pair distribution functions of 2D projections

We can use the results obtained above to derive the 2D projection PDF, $g_P(\tilde{r}_{12})$, expected for particular forms of the isotropic 3D structure PDF, $g(r_{12})$. Amorphous structures have no long range order, and

$$g(r_{12}) = 1$$

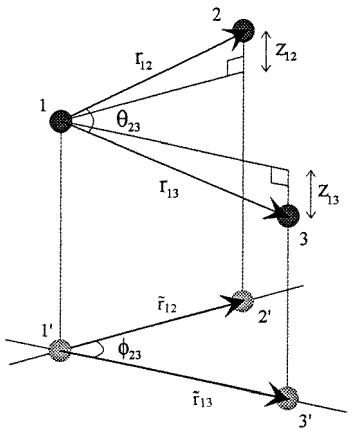

Figure 1. Variables used to describe the positions of triplets of atoms (1, 2 and 3) in a 3D structure and particles (1′, 2′ and 3′) in the corresponding 2D projection.

for large r_{12}. Inserting this into equation (10) gives

$$g_P(\tilde{r}_{12}) = \frac{2}{t}\int_0^t \left(1 - \frac{z_{12}}{t}\right) \mathrm{d}z_{12} = \frac{2}{t}\left[z_{12} - \frac{z_{12}^2}{2t}\right]_0^t = 1$$

i.e. the projection also has no long range order, as expected. This result is independent of t because the value of the integral over z_{12} increases with t, and exactly balances the t^{-1} factor in front of the integral. Amorphous structures also have non-overlapping atoms, i.e. $g(r_{12}) = 0$ for $r < R1$, where $R1$ is the nearest neighbour distance. Taking

$$g(r_{12}) = 0 \text{ for } r_{12} < R1 \text{ and } g(r_{12}) = 1 \text{ for } r_{12} \geqslant R1$$

i.e. a step function in r_{12}, is equivalent to carrying out the previous integral with the condition $(\tilde{r}_{12}^2 + z_{12}^2)^{0.5} \geqslant R1$ or $z_{min} = (R1^2 - \tilde{r}_{12}^2)^{0.5}$, which gives

$$g_P(\tilde{r}_{12}) = \frac{2}{t}\left[z_{12} - \frac{z_{12}^2}{2t}\right]_{z_{min}}^t = 1 - \frac{2}{t}\left(z_{min} - \frac{z_{min}^2}{2t}\right) = \left(1 - \frac{z_{min}}{t}\right)^2$$
$$= (1 - (R1^2 - \tilde{r}_{12}^2)^{0.5})^2$$

for $\tilde{r}_{12} < R1$, and equal to 1 for $\tilde{r} \geqslant R1$. Finally, the short range order in amorphous structures includes a nearest neighbour peak of $N1$ atoms at a distance of $R1$. A simple approximation for this is

$$g(r_{12}) = \frac{N1}{4\pi R1^2 \rho_0}\delta(r_{12} - R1). \tag{13}$$

Because of the delta function in r_{12}, it is helpful to change the variable of integration from z_{12} to $r_{12} = (\tilde{r}_{12}^2 + z_{12}^2)^{0.5}$, which gives

$$g_P(\tilde{r}_{12}) = \frac{2}{t}\int_0^t \left(1 - \frac{z_{12}}{t}\right) g(r_{12}) \frac{r_{12}}{(r_{12}^2 - \tilde{r}_{12}^2)^{0.5}} \mathrm{d}r_{12}$$
$$= \left(1 - \frac{(R1^2 - \tilde{r}_{12}^2)^{0.5}}{t}\right) \frac{N1}{2\pi R1^2 \rho_{0P}} \frac{R1}{(R1^2 - \tilde{r}_{12}^2)^{0.5}}$$

for $\tilde{r}_{12} \leqslant R1$, and equal to 0 for $\tilde{r} > R1$. The first factor takes account of finite thickness of the 3D structure, and the remaining factors are equal to the projection of the spherical shell described by equation (13).

Using the above components, we have constructed a form of $g(r_{12})$ which approximates that for tetrahedral amorphous carbon. It has a sharp nearest neighbour peak at $R1 = 1.5$ Å with $N1 = 4$, a broad second nearest neighbour peak from 2.3 to 2.7 Å, and no ordering at larger distances. This is shown in figure 2, along with the corresponding form of $g_P(\tilde{r}_{12})$ for thickness $t = 20$ Å. We have not attempted an analogous procedure with the TDFs, because of the greater complexity of those functions.

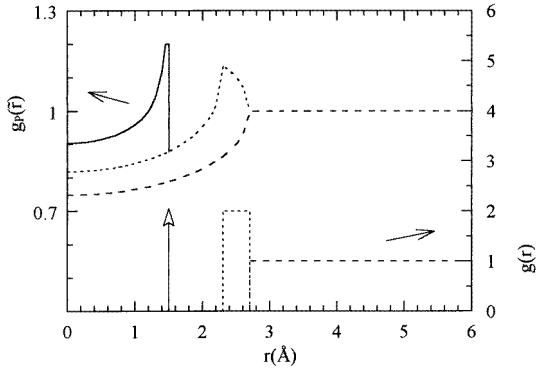

Figure 2. Approximation to $g(r)$ (lower lines) and corresponding analytic form of $g_P(\tilde{r})$ (upper lines) for ta-C with $t = 20$ Å.

3. Results from calculations

3.1. 3D structure models used

In the previous section, we showed that the order in a 2D projection is a function of the order in the corresponding 3D structure. To verify the relationships derived, we have carried out calculations of distribution functions for actual 3D structures and their corresponding 2D projections. The 3D structures we have used are atomic models of tetrahedral amorphous carbon, ta-C. These models were made available to us by K W R Gilkes who developed them by adapting earlier models of amorphous silicon [20–22]. For our purposes, we simply require structures which are representative of amorphous solids, i.e. they have well defined short range order and no long range order. Whether or not these models are entirely accurate representations of the structure of ta-C is not relevant. However, we note that work on HREM of thin amorphous structures often involves samples of amorphous Si or Ge, and it is reasonable to consider that ta-C belongs to the same general class of materials.

We have used three different models of ta-C which all have cubic periodic boundary conditions with atomic density $\rho_0 = 0.17$ atoms Å^{-3}. The three models have box lengths $L = 10.6$ Å, $L = 18.05$ Å and $L = 43.3$ Å, and numbers of atoms $N = 216$, $N = 1000$ and $N = 13\,810$ (respectively). For simplicity, 2D projections were obtained from the models in the directions of the x, y and z axes, corresponding to coordinates (Y_i, Z_i), (Z_i, X_i) and (X_i, Y_i) respectively. These projections have $t = L$, and have square periodic boundary conditions with box length L. (Note that smaller thicknesses and/or different orientations could be obtained by choosing appropriate subsets of the model coordinates.)

3.2. Direct calculations of 3D structure distribution functions

The pair distribution functions (PDFs) for the 3D structures have been obtained by direct calculation from the coordinates of the 3D models using equations (1)–(3). Calculations of the 3D structure distribution functions are non-redundant for interatomic distances less than $L/2$. The 3D structure PDFs, $g(r_{12})$, are shown in figures 3 and 4 for the models of ta-C with $L = 18.05$ and $L = 43.3$ Å, with distance intervals of 0.06 Å. The triplet distribution functions (TDFs) for the 3D structures have been obtained by direct calculation from the coordinates of the 3D models using equations (4)–(6). The 3D structure TDFs, $g3(r_{12}, r_{23}, \theta_{23})$, are shown in figures 5 and 6 for the models of ta-C with $L = 10.6$ and $L = 18.05$ Å, with distance intervals of 0.2 Å and angle intervals of 10°. The TDF was not calculated for the model with $L = 43.3$ Å because it would require too much computing time.

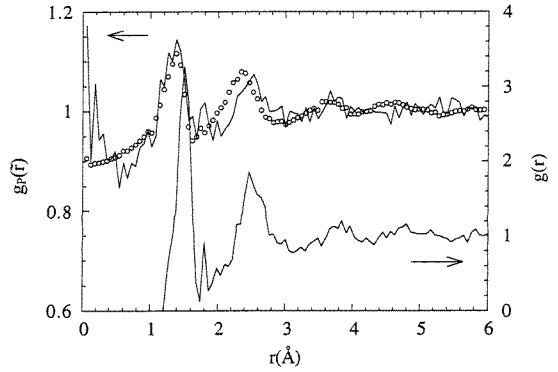

Figure 3. Direct calculation of $g(r)$ (lower line) and $g_P(\tilde{r})$ (upper line), and numerical integration calculation of $g_P(\tilde{r})$ (circles) for model of ta-C with $N = 1000$ and $t = 18.05$ Å.

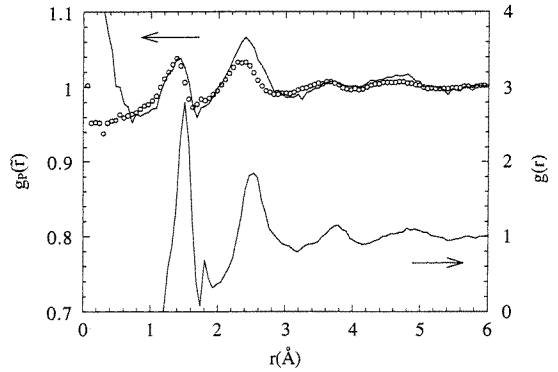

Figure 4. Direct calculation of $g(r)$ (lower line) and $g_P(\tilde{r})$ (upper line), and numerical integration calculation of $g_P(\tilde{r})$ (circles) for model of ta-C with $N = 13\,810$ and $t = 43.3$ Å.

The function $g3(r_{12}, r_{23}, \theta_{23})$ depends on three variables and hence a single figure can only show a limited range of the values of the function. The method we have chosen is a contour plot with the height of contours representing the values of the function (see table 1). The variable r_{12} is fixed equal to 1.6 Å, corresponding to arrangements of triplets of atoms

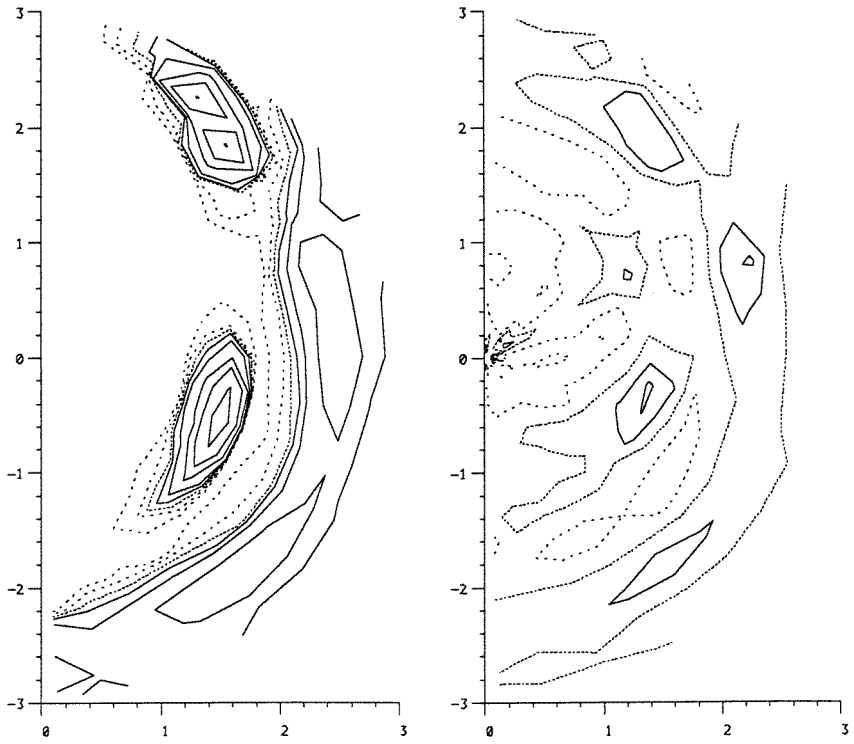

Figure 5. Direct calculation of $g3(r_{12}, r_{23}, \theta_{23})$ (left) and $g3_P(\tilde{r}_{12}, \tilde{r}_{23}, \phi_{23})$ (right) for a model of ta-C with $N = 216$ and $t = 10.6$ Å, for values of $r_{12} = 1.6$ Å and $\tilde{r}_{12} = 1.6$ Å. The dependent variables are shown in rectangular coordinates. The values of contours are given in table 1.

Table 1. Values of contours in plots of triplet distribution functions.

Figure	Model	Dotted lines	Dashed line	Solid lines
5 (left)	$t = 10.6$ Å, 3D structure	0.1, 0.5	1.0	1.5, 2.5, 5, 10, 20
6 (left)	$t = 18.1$ Å, 3D structure	0.1, 0.5	1.0	1.5, 2.5, 5, 10, 20
5 (right)	$t = 10.6$ Å, 2D projection	0, 0.2, . . . , 0.8	1.0	1.2, 1.4, . . . , 3.0
6 (right)	$t = 18.1$ Å, 2D projection	0.75, 0.80, . . . , 0.95	1.0	1.05, 1.10, . . . , 1.50

containing nearest neighbour atoms. The plane of plotting represents the dependent variables r_{13} and θ_{23}, shown in rectangular coordinates, which describe the position of particle 3 relative to particles 1 and 2 (see figure 1). Particle 1 is located at the origin and particle 2 is located on the positive vertical axis at distance r_{12} from the origin. (Similar comments apply to the plots of the 2D projection TDFs.)

Because TDFs are not commonly reported functions we will briefly discuss their interpretation. The 3D structure TDF, $g3(r_{12}, r_{23}, \theta_{23})$, shows the frequency of different arrangements of triplets of atoms. In a ta-C structure, the most common arrangement of triplets of atoms will be three carbon atoms forming a tetrahedral bond, i.e. r_{12} and r_{13} equal to approximately 1.54 Å, and θ_{23} equal to approximately 109°. Figures 5 and 6 show the results for $g3(r_{12}, r_{23}, \theta_{23})$ with $r_{12} = 1.6$ Å, and as expected there is a peak at $r_{13} = 1.6$ Å and

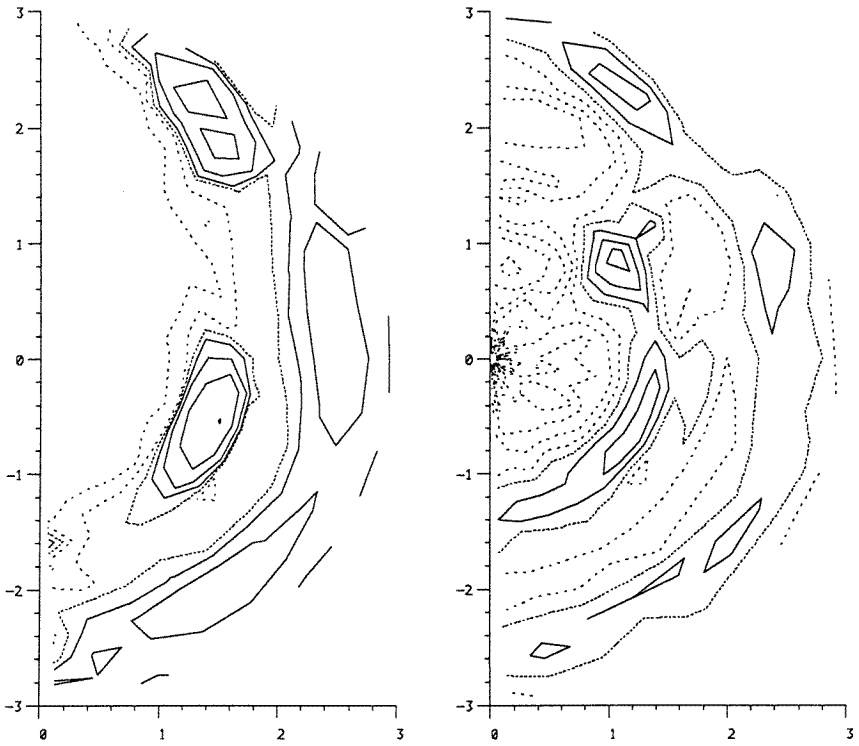

Figure 6. Direct calculation of $g3(r_{12}, r_{23}, \theta_{23})$ (left) and $g3_P(\tilde{r}_{12}, \tilde{r}_{23}, \phi_{23})$ (right) for a model of ta-C with $N = 1000$ and $t = 18.05$ Å, for values of $r_{12} = 1.6$ Å and $\tilde{r}_{12} = 1.6$ Å. The dependent variables are shown in rectangular coordinates. The values of contours are given in table 1.

$\theta_{23} = 110^\circ$. The same arrangement of atoms, but with the labels of atoms 1 and 2 exchanged, also gives a peak at $r_{13} = 2.5$ Å and $\theta_{23} = 35^\circ$, also seen in figures 5 and 6. TDFs are of significant interest for improving our ability to describe and understand amorphous structures [15]. We will discuss them further in a future paper.

3.3. Direct calculation of 2D projection distribution functions

The PDFs and TDFs for 2D projections have been obtained by direct calculation from the coordinates of the projection using the 2D equivalents of the equations used for the 3D structure, e.g. equations (7) and (8). Calculations of the 2D projection distribution functions are non-redundant for interatomic distances less than $L/2$. The 2D projection PDFs, $g_P(\tilde{r}_{12})$, are shown in figures 3 and 4 for the models of ta-C with $L = 18.05$ and $L = 43.3$ Å, with distance intervals of 0.06 Å. The results presented are the averages for the three different projections perpendicular to the x, y and z axes. Figures 3 and 4 also show the estimates of $g_P(\tilde{r}_{12})$ obtained by numerical integration of equation (10) using the values of $g(r_{12})$.

The 2D projection TDFs, $g3_P(\tilde{r}_{12}, \tilde{r}_{23}, \phi_{23})$, are shown in figures 5 and 6 for the models of ta-C with $L = 10.6$ and $L = 18.05$ Å, with distance intervals of 0.2 Å and angle intervals of 10°. The results obtained are the averages for the three different projections perpendicular to the x, y and z axes. (The format of the plots is described in the previous section.)

4. Discussion

4.1. Order in projections

We have shown that the pair distribution function (PDF) of a 2D projection, $g_P(\tilde{r}_{12})$, is a function of the PDF of the corresponding 3D structure, $g(r_{12})$, and similarly for the triplet distribution functions (TDFs), $g3_P(\tilde{r}_{12}, \tilde{r}_{23}, \phi_{23})$ and $g3(r_{12}, r_{23}, \theta_{23})$ (respectively). Inspection of the relationships in equations (10) and (12) reveals the following characteristics:

(i) Order occurs in a 2D projection because applying an integral over $\mathrm{d}z$ to an isotropic structure gives higher weighting to interatomic vectors which are nearly perpendicular to the direction of projection, so that their projected vectors will be similar.

(ii) A feature localized at $r_{12} = R1$ in $g(r_{12})$ gives a contribution in $g_P(\tilde{r}_{12})$ at values of $\tilde{r}_{12} \leqslant R1$. Similarly, a feature localized at $r_{12} = R1$, $r_{13} = R1'$ and $\theta_{23} = \Theta 1$ in $g3(r_{12}, r_{23}, \theta_{23})$ gives a contribution in $g3_P(\tilde{r}_{12}, \tilde{r}_{23}, \phi_{23})$ at values of $\tilde{r}_{12} \leqslant R1$, $\tilde{r}_{13} \leqslant R1'$ and $\phi_{23} \leqslant \Theta 1$.

(iii) If the 3D structure PDF can be written as a sum of several different components (e.g. first and second nearest neighbour peaks), then the 2D projection PDF will be equal to the sum of the contributions from the different components. This characteristic is quite clear in figure 2. The same is true for TDFs. In this respect, the relationship between 3D structure and 2D projection distribution functions is 'linear'.

(iv) The effect of increasing thickness is to diminish the degree of order in the 2D projection, due to factors of t^{-1} in equation (10) and t^{-2} in equation (12), for the 2D projection PDF and TDF respectively.

These characteristics can be seen in the directly calculated results for $g_P(\tilde{r}_{12})$ which are shown in figures 3 and 4. There are small peaks corresponding to the first and second nearest neighbour distances at approximately 1.5 and 2.5 Å respectively. Comparison of figures 3 and 4, for 2D projections with $t = 18.05$ and $t = 43.3$ Å respectively, confirms that the size of features is proportional to t^{-1}. Furthermore, there is good agreement between the $g_P(\tilde{r}_{12})$ calculated directly, and those estimated by numerical integration of $g(r_{12})$ using equation (10).

The qualitative correspondence between features in $g3_P(\tilde{r}_{12}, \tilde{r}_{23}, \phi_{23})$ and those in $g3(r_{12}, r_{23}, \theta_{23})$ is apparent in figures 5 and 6. In particular, there are clearly small peaks in $g3_P(\tilde{r}_{12}, \tilde{r}_{23}, \phi_{23})$ at $\tilde{r}_{12} = 1.5$ Å and $\phi_{23} = 110^\circ$, and at $\tilde{r}_{13} = 2.5$ Å and $\phi_{23} = 35^\circ$, which correspond to triplets of carbon atoms forming tetrahedral bonds. Comparison of figures 5 and 6, for 2D projections with $t = 10.6$ and $t = 18.05$ Å respectively, confirms that the strength of features decreases as t increases. From inspection of the figures, the average ratio of the peak heights is approximately 3:1 which is consistent with a t^{-2} dependence.

4.2. Signal to noise

The results from the theory section make particular predictions about the effect of t on the degree of order in the 2D projections. To better understand the effects of thickness, we can consider the PDF as the sum of a random component, equal to 1, and the remainder, $g(r_{12}) - 1$. As discussed previously, the random component is independent of thickness. The value of $g(r_{12}) - 1$ is only significantly different from zero for small values of r_{12} and hence z_{12}. Because of this, the value of the integral over $\mathrm{d}z_{12}$ in equation (10) does not increase with t, and the t^{-1} factor in front of the integral determines the t dependence. Similar comments apply to the TDF, except that there is a t^{-2} factor due to the double integral.

While the signal can be taken to be the degree of order in the 2D projection, it is also important to consider the noise. If we regard the ta-C models as complete structures in themselves,

then the results presented are 'exact' because they were calculated directly from the model coordinates. However, if we regard the ta-C models as subsets of (hypothetical) infinite 3D structures, then the results have statistical uncertainties due to sampling over a limited volume and hence N. For a 2D projection with N particles each with $N1$ nearest neighbour particles, the counting noise will be $(NN1)^{0.5}$ for the PDF, and $(N \times N1(N1-1)/2)^{0.5}$ for the TDF. Furthermore, the value of N increases as t. Hence, we estimate that the signal to noise ratio in the 2D projection, denoted 'S/N', has a t dependence of t^0 for the PDF and $t^{-0.5}$ for the TDF.

However, the effect of noise which increases with t can be reduced by increasing the area of the $2D$ projection and hence N. Because our models are cubic, the area increases as t^2, and N increases as t^3. Hence we estimate that the S/N for our results has a t dependence of t^1 for the PDF and $t^{0.5}$ for the TDF. These results may seem surprising, but inspection of figures 3, 4, 5 and 6 reveals that the S/N does not decrease even though the thickness increases by a factor of 2. Note that our discussion here is concerned with ideal 2D projections, and not with any possible experimental observations. Another factor to consider is that the TDF is a much sharper function than the PDF [15], and this may partly offset the less favourable t dependence.

4.3. Unusual features in the 2D projection distribution functions

Figures 3 and 4 show the $g_P(\tilde{r}_{12})$ calculated directly, along with those estimated by numerical integration of $g(r_{12})$. While there is good agreement overall, the agreement is not completely within the level of noise. We consider one reason for this to be because the direct calculation was only for projections in directions parallel to the x, y and z axes, whereas the numerical integration was based on the isotropic $g(r_{12})$. These will only be the same if the structure is entirely isotropic, and the small amount of disagreement indicates to us that this is not the case. In fact, for the model with $t = 43.3$ Å, there is a very large discrepancy in the form of a peak for values of $\tilde{r}_{12}$ tending to zero. This does not occur in the numerical integration, and cannot because there is no feature in $g(r_{12})$ for values of r_{12} tending to zero. As the starting configuration of this model was an FCC structure [20], we consider it feasible that the artefact in the 2D projection PDF represents anisotropy in the model in the directions parallel to the x, y and z axes due to a remnant of the initial FCC structure. Note that there appears to be a similar artefact for the $t = 18.05$ Å model, and it also had an FCC starting configuration [21].

Figures 5 and 6 show the results for TDFs. There is a peak in $g3_P(\tilde{r}_{12}, \tilde{r}_{23}, \phi_{23})$ at $\tilde{r}_{13} = 1.4$ Å and $\phi_{23} = 55^\circ$ which has no counterpart in $g3(r_{12}, r_{23}, \theta_{23})$. Indeed, it cannot because the 3D structure does not contain bond angles of 55°. This feature is an artefact of the kind which can arise in the higher order distribution functions of 2D projections. Its specific origin is indicated in figure 7. When a triplet of carbon atoms forming a tetrahedral bond is projected so that the second nearest neighbour atoms appear to be separated by the nearest neighbour distance, the central atom will be projected to an intermediate position. The angular average of possible orientations gives rise to the peak observed. This serves to reiterate the role which angular averaging plays in 'transmitting' order from the 3D structure to the 2D projection.

4.4. Distribution functions with more dependent variables

The results presented here have dealt only with isotropic distribution functions. These are simpler to calculate because they have fewer dependent variables. They are also appropriate for large models of bulk amorphous structures which are expected to be isotropic. However, we have seen that even a model with $L = 43.3$ Å shows signs of anisotropy. While this may be an attribute of the particular model, the question as to whether amorphous solids in general are isotropic on small length scales is a subject of considerable interest (see e.g. [14]). Indeed, if

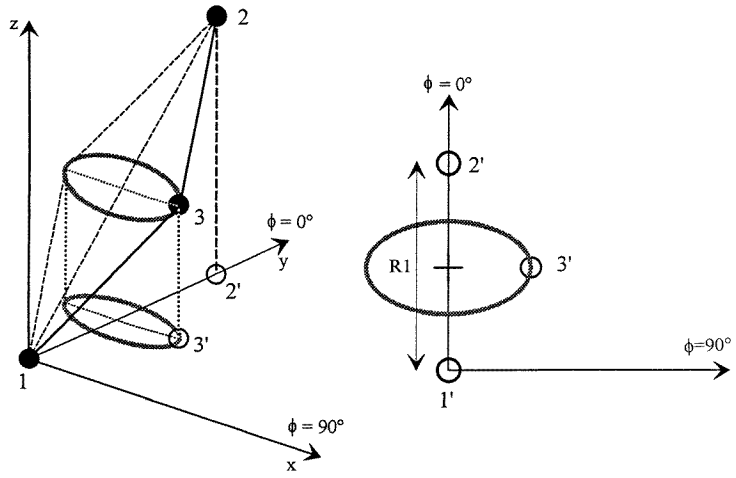

Figure 7. Origin of the artefact appearing in 2D projection TDF $g3_P(\tilde{r}_{12}, \tilde{r}_{23}, \phi_{23})$ for models of ta-C, for values of $\tilde{r}_{12} = 1.6$ Å.

there is small scale isotropy in thin amorphous structures, we consider it likely to be apparent in their projections. Hence it is of interest to consider the anisotropic distribution functions, i.e. without radial averaging. These have the same relationships as those for the isotropic distribution functions (see equations (10) and (12)).

This work has considered only monatomic structures. For 3D structures with more than one kind of atom, the use of partial distribution functions is well established. These distinguish the correlations according to the type of atom involved [16]. All of the results presented here are capable of extension in this way.

From the equations presented for PDFs and TDFs, it is seen to be a straightforward matter to derive results for higher order correlation functions, e.g. an n-tuplet distribution function. While this may not be practical due to the complexity of the dependent variables (which have $3n - 6$ dimensions for isotropic n-tuplets), it is important for understanding the order in 2D projections of amorphous 3D structures. A 2D projection contains information about all higher order correlations because it preserves local information about the 3D structure, i.e. (X_i, Y_i), but the information is diminished by factors t^{1-n}. This can be compared with diffraction which only gives information about PDFs.

4.5. The relationship between 2D projections and diffraction

We have discussed the relationship between 2D projections and 3D structures in terms of distribution functions. We now consider the relationship in terms of the techniques which can be used to obtain information about these functions. The use of diffraction to measure the PDF of amorphous 3D structures is a well established technique. In favourable circumstances the isotropic PDF can be measured with a resolution of 0.02 Å. It is instructive to make a comparison with the information about the PDF which underlies HREM.

In a diffraction experiment, the scattering of incident radiation is measured as a function of the scattering vector $\boldsymbol{q} = \Delta\boldsymbol{k}$, where $\boldsymbol{k}$ is the wavevector. The relative phase shift of scattering from point $\boldsymbol{r}$ in the 3D structure is $\exp(\mathrm{i}\boldsymbol{q}\cdot\boldsymbol{r})$. In the first Born approximation [23], the amplitude of scattering is

$$A(\boldsymbol{q}) = f(\boldsymbol{q})\mathrm{FT}_{3d}^{-1}\{\rho(\boldsymbol{r})\}$$

where $f(\boldsymbol{q})$ describes the scattering from an atom due to the atomic potential, and FT denotes the Fourier transform operation. Thus the scattering amplitude is a function of $\rho(\boldsymbol{r})$ which contains all structural information. However, the quantity measured is the scattering intensity,

$$I(\boldsymbol{q}) = |f(\boldsymbol{q})|^2 \mathrm{FT}_{3d}^{-1}\{N(\rho_0 g(\boldsymbol{r}_{12}) + \delta(\boldsymbol{r}_{12}))\}$$

which only contains information about the PDF (because squaring the amplitudes is equivalent to taking the autocorrelation of $\rho(\boldsymbol{r})$) [16]. For an isotropic 3D structure the 3D inverse Fourier transform becomes a 1D integral,

$$\frac{1}{2\pi^2}\int\left(\frac{I(q)}{|f(q)|^2}\right)\sin(qr)q^2\,\mathrm{d}q = N(\rho_0 g(r_{12}) + \delta(r_{12})). \tag{14}$$

In the case of electron diffraction in a transmission electron microscope, the scattering is measured in the $\tilde{\boldsymbol{q}}$ plane, where $\tilde{\boldsymbol{q}}$ is the 2D vector (q_x, q_y). By a standard theorem, the value of the Fourier transform in a plane through the origin is equal to the Fourier transform of the projection in the direction perpendicular to the plane [24]. Hence, the scattering amplitude in the $\tilde{\boldsymbol{q}}$ plane,

$$A(\tilde{\boldsymbol{q}}) = f(\tilde{\boldsymbol{q}})\mathrm{FT}_{2d}^{-1}\left\{\int \rho(\boldsymbol{r})\,\mathrm{d}z\right\}$$

depends only on the projected particle density function. If the 3D structure is not isotropic, the information about the 2D projection PDF is obtained from the scattering intensity,

$$I(\tilde{\boldsymbol{q}}) = |f(\tilde{\boldsymbol{q}})|^2 \mathrm{FT}_{2d}^{-1}\{N(\rho_{0P} g_P(\tilde{\boldsymbol{r}}_{12}) + \delta(\tilde{\boldsymbol{r}}_{12}))\}.$$

For an isotropic 3D structure the 2D inverse Fourier transform becomes a 1D integral,

$$\frac{1}{2\pi}\int\left(\frac{I(q)}{|f(q)|^2}\right)J_0(qr)q\,\mathrm{d}q = N(\rho_{0P} g_P(\tilde{r}_{12}) + \delta(\tilde{r}_{12})) \tag{15}$$

where J_0 is a Bessel function [25]. For an isotropic structure $I(\boldsymbol{q}) = I(\tilde{\boldsymbol{q}}) = I(q)$, and the structural information in $g(r_{12})$ and $g_P(\tilde{r}_{12})$ is equivalent because both equations (14) and (15) are functions of $I(q)$. Note also that whereas the relationship between $I(q)$ and $g(r_{12})$ is independent of t because ρ_0 is independent of t, $g_P(\tilde{r}_{12})$ has a t^{-1} dependence on $I(q)$ due to the factor ρ_{0P} in equation (15).

In the case of standard HREM, the scattering amplitude in the diffraction plane, $A(\tilde{\boldsymbol{q}})$, passes through an electron lens which focuses it into an image in the image plane [1]. An additional phase shift occurs due to lens aberrations, described by the contrast transfer function $\chi(\tilde{\boldsymbol{q}})$. Hence the $\tilde{\boldsymbol{q}}$ dependence of the image amplitude is

$$A'(\tilde{\boldsymbol{q}}) = \delta(\tilde{\boldsymbol{q}}) - \mathrm{i}\exp(\mathrm{i}\chi(\tilde{\boldsymbol{q}}))f(\tilde{\boldsymbol{q}})\mathrm{FT}_{2d}^{-1}\{\rho_P(\tilde{\boldsymbol{r}})\} \tag{16}$$

where $\delta(\tilde{\boldsymbol{q}})$ is the unscattered beam. In the weak phase object approximation, the image contrast is dominated by the interference of the left and right terms in equation (16), i.e. it is linear in $\mathrm{FT}_{2d}^{-1}\{\rho_P(\tilde{\boldsymbol{r}})\}$. In the first approximation, $\chi(\tilde{\boldsymbol{q}})$ acts as a frequency filter with reverse contrast. The important point is the preservation of the phase information in $A'(\tilde{\boldsymbol{q}})$ (which does not occur in diffraction) and thereby the information about $\rho_P(\tilde{\boldsymbol{r}})$, and hence the 2D projection PDF, TDF and higher order correlations.

5. Conclusions

We have examined the order in 2D projections of 3D amorphous structures using distribution functions, and have derived the relationships between the pair distribution functions (PDFs) of the 3D structure and of the corresponding 2D projection. Analogous relationships have been

obtained for the triplet distribution functions (TDFs). We have confirmed the relationships in the case of isotropic distribution functions using calculations on models of an amorphous solid (ta-C) with thicknesses, t, in the range from 10.6 to 43.3 Å. The 2D projection PDF and TDF show small peaks corresponding to the peaks in the 3D structure PDF and TDF, such as for nearest neighbours and tetrahedral bonding, respectively. The degree of order in the 2D projection is diminished as t increases, with a dependence of t^{-1} for the PDF and t^{-2} for the TDF. However, this effect can be offset by using larger areas of projection, and peaks in the 2D projection PDF were quite clear for $t = 43.3$ Å. Deviations in the 2D projection PDF from that expected for an isotropic structure gives evidence of anisotropy in the models. The 2D projection TDF shows a peak which does not correspond to those in the 3D structure TDF and which represents an artefact that can occur in the higher order correlations of 2D projections. The same approach can be extended to higher order correlation functions than the TDF. Thus it has been demonstrated that 2D projections of 3D amorphous structures contain a great deal of valuable structural information. From this point of view, the possibility of improvements in electron microscopy techniques leading to sub-Å resolution HREM images of amorphous materials is an exciting prospect.

Acknowledgments

I would like to thank J R Rodenburg for useful discussions, K W R Gilkes for the use of models, S J Brown for assistance with figures and P H Gaskell for his supervision. This work was sponsored by the Commonwealth Scholarships Commission, Association of Commonwealth Universities.

References

[1] Spence J C H 1980 *Experimental High Resolution Electron Microscopy* (Oxford: Clarendon)
[2] Lichte H 1991 *Adv. Opt. Electron Microsc.* **12** 25
[3] Orchowski A, Rau W D and Lichte H 1995 *Phys. Rev. Lett.* **74** 399
[4] Van Dyck D, Op de Beeck M and Coene W 1993 *Optik* **93** 103
[5] Pennycook S J and Jesson D E 1990 *Phys. Rev. Lett.* **64** 938
[6] Krivanek O L, Dellby N, Spence A J, Camps R A and Brown L M 1997 *EMAG 1997 (IOP Conf. Ser. 153)* ed J M Rodenburg (Bristol: Institute of Physics) p 35
[7] Nellist P D, McCallum B C and Rodenburg J M 1995 *Nature* **374** 630
[8] Rodenburg J M and Bates R H T 1992 *Phil. Trans. R. Soc.* A **339** 521
[9] Howie A 1978 *J. Non-Cryst. Solids* **31** 41
[10] Gaskell P H 1988 *Electron Beam Imaging of Non-Crystalline Materials (IOP Short Meetings Ser. 11)* (Bristol: Institute of Physics) p 47
[11] Bursill L A, Mallinson L G, Elliot S R and Thomas J M 1981 *J. Phys. Chem.* **85** 3004
[12] Gibson J M 1994 *Ultramicroscopy* **56** 26
[13] Kirvanek O L, Gaskell P H and Howie A 1976 *Nature* **262** 454
[14] Gaskell P H and Wallis D J 1996 *Phys. Rev. Lett.* **76** 66
[15] Mountjoy G 1995 *PhD Thesis* University of Cambridge
[16] Cusack N E 1987 *The Physics of Structurally Disordered Matter* (Bristol: Hilger) p 30
[17] Filipponi A, Dicicco A and Natoli C R 1995 *Phys. Rev.* B **52** 15 122
[18] Steinhardt P J, Nelson D R and Ronchetti M 1983 *Phys. Rev.* B **28** 784
[19] Lohmann A W and Wirnitzer B 1984 *Proc. IEEE* **72** 889
[20] Holender J and Morgan G J 1991 *J. Phys.: Condens. Matter* **3** 1947
[21] Wooten F and Weaire D 1984 *J. Non-Cryst. Solids* **106** 1
[22] Wooten F, Winder K and Weaire D 1985 *Phys. Rev. Lett.* **54** 1392
[23] Schiff L I 1968 *Quantum Mechanics* (New York: McGraw-Hill) p 324
[24] Cowley J M 1981 *Diffraction Physics* (Amsterdam: North-Holland)
[25] Gaskill J D 1978 *Linear Systems, Fourier Transforms, and Optics* (New York: Wiley) p 317